

PAPER • OPEN ACCESS

Rotation in galaxy clusters from MUSIC simulations with the kinetic Sunyaev–Zel’dovich effect

To cite this article: A S Baldi *et al* 2019 *J. Phys.: Conf. Ser.* **1226** 012003

View the [article online](#) for updates and enhancements.



IOP | ebooks™

Bringing you innovative digital publishing with leading voices to create your essential collection of books in STEM research.

Start exploring the collection - download the first chapter of every title for free.

Rotation in galaxy clusters from MUSIC simulations with the kinetic Sunyaev–Zel’dovich effect

A S Baldi¹, M De Petris¹, F Sembolini^{1,2}, G Yepes², W Cui², L Lamagna¹

¹ Dipartimento di Fisica, Sapienza Università di Roma, Piazzale Aldo Moro 5, I-00185 Roma, Italy

² Departamento de Física Teórica, Universidad Autónoma de Madrid, Calle Francisco Tomás y Valiente 7, E-28049 Madrid, Spain

E-mail: annasilvia.baldi@uniroma1.it

Abstract. The Sunyaev–Zel’dovich effect in galaxy clusters is a unique probe for studying astrophysics and cosmology. We propose in this work its application for the detection of possible coherent rotational motions in the hot intra-cluster medium. We select a sample of massive, relaxed and rotating galaxy clusters from Marenostrum-mUltidark SIMulations of galaxy Clusters (MUSIC), and we produce mock maps of the temperature distortion produced by the kinetic Sunyaev–Zel’dovich effect by exploring six different lines of sight, in the best observational condition. These maps are compared with the expected signal computed from a suitable theoretical model in two cases: (*i*) focusing only on the contribution from the rotation, and (*ii*) accounting also for the cluster bulk motion. We find that the parameters of the model assumed for the radial profile of the rotational velocity, averaged over the considered lines of sight, are in agreement within two standard deviations at most with independent estimates from the simulation data, without being significantly affected by the presence of the cluster bulk term. The amplitude of the rotational signal is, on average, of the order of 23 per cent of the total signal accounting also for the cluster bulk motion, and its values are consistent with the literature. The projected bulk velocity of the cluster is also recovered at the different lines of sight, with values in agreement with the simulation data.

1. Introduction

The study of non-random motions in the diffuse gas in galaxy clusters (the intra-cluster medium, or ICM) can play an important role for precision cosmology. Indeed, cluster masses are a valuable observable for constraining some cosmological parameters, and accurate mass measurements should take into account the contribution from possible ordered motions, which would be given by an effective non-thermal pressure gradient [1]. Recent results from hydrodynamical simulations have shown, indeed, that mass estimates accounting only for the support from thermal pressure are generally biased towards values 10-20 per cent lower than the true ones (see e.g. [2] and references therein). With the aim of quantifying the non-thermal correction to the hydrostatic mass, several approaches have been proposed to detect, in particular, possible ordered *rotational* motions in the ICM, through observations of the ICM itself or of the galaxy members at X-ray [3], millimetre [4–6], and optical wavelengths [7–9].



In this work, we focus on the detection of a possible rotation of the ICM based on measurements in the microwave band of the kinetic component of the Sunyaev–Zel’dovich (SZ) effect [10, 11]. The SZ effect arises from the Comptonization of the photons of the cosmic microwave background (CMB), as they propagate through galaxy clusters and interact with the free electrons in the ICM. The scattering causes the redistribution of the energy of the photons, which can be measured as an intensity (or temperature) distortion of the CMB blackbody spectrum. Two components can be distinguished in the SZ effect: one is due to the thermal motion of the electrons (the thermal SZ effect, tSZ); the other one is produced by the motion of the cluster as a whole with respect to the CMB rest frame (the kinetic SZ effect, kSZ). Since it is proportional to the ICM velocity, the kSZ can be a useful probe of cluster dynamics. In particular, a purely rotational motion of the ICM would be detectable from the kSZ temperature distortion, which is expected to feature a dipole pattern, due to the projected approaching and receding velocities of the rotating gas relatively to the observer, as investigated in [4] and [5] for the first time.

Synthetic galaxy clusters from large cosmological hydrodynamical simulations represent ideal targets for preliminary studies on the feasibility of the detection of a rotation with the aforementioned possible observational strategies. The MUSIC¹ catalogue [12] is one of the largest data set of simulated galaxy clusters to date. We select six candidate rotating clusters from MUSIC according to the results we reported in a companion paper [13], and we produce numerical maps of the kSZ temperature signal. In order to constrain their rotation, we fit them to the expected theoretical kSZ maps for a rotating ICM. In particular, we assume the model by [4] as a starting basis, and we update it by accounting for a different law describing the rotational velocity we proposed in [13], assuming both a rotation-only case, and the full case accounting also for the cluster bulk motion.

The paper is organized as follows. Sec. 2 briefly reports the features of our cluster data set. In Sec. 3 we describe the theoretical and mock kSZ temperature maps. In Sec. 4 we report our results, and eventually we summarize our conclusions in Sec. 5.

2. Data set

We select our target clusters from the MUSIC-2 catalogue which is based on high-resolution re-simulations of clusters from the MultiDark parent simulation [14], from which we also inherit the assumed cosmological model (see [12] for details). Simulations are run with the GADGET-3 Tree-PM+SPH (i.e. using particle-mesh and smoothed particle hydrodynamics) code, and follow the evolution of gas and dark matter particles, which have masses $m_{\text{gas}} = 1.9 \times 10^8 h^{-1} M_{\odot}$ and $m_{\text{DM}} = 9.0 \times 10^8 h^{-1} M_{\odot}$, respectively (where M_{\odot} is the mass of the sun and $h = 0.7$). For our purposes of studying rotation, we focus in particular on a sample of massive (virial masses $M_{\text{vir}} > 5 \times 10^{14} h^{-1} M_{\odot}$), dynamically relaxed objects at redshift $z = 0$, with spin parameter of the gas $\lambda_{\text{gas}} > 0.07$ (see the companion work by [13] for further details). The main properties of our cluster sample selected according to these criteria are summarized in Tab. 1. We limit our present analysis to objects extracted from the adiabatic run, i.e. without accounting for radiative baryon physics processes, since they do not have significant impact on the rotational properties of the gas [13].

¹ <http://music.ft.uam.es>

Table 1. Identifier, virial mass, virial radius and spin parameter of the gas of the six galaxy clusters analysed in this work.

cluster ID	$M_{\text{vir}} (\times 10^{15} M_{\odot})$	$R_{\text{vir}} (\text{kpc})$	λ_{gas}
46	1.17	2756	0.0785
93	1.90	3241	0.0769
98	1.61	3071	0.0735
103	1.02	2633	0.0746
205	1.24	2813	0.0763
256	1.31	2867	0.0714

3. Maps of the kSZ effect

3.1. Theoretical model maps

The map of the kSZ temperature distortion produced by the rotation of the ICM described by a generic angular velocity law $\omega(r)$, can be written as [4]:

$$\frac{\Delta T_{\text{kSZ},r}(R, \phi)}{T_{\text{CMB}}} = -\frac{\sigma_T}{c} R \cos \phi \sin i \int_R^{R_{\text{vir}}} n_e(r) \omega(r) \frac{2r dr}{\sqrt{r^2 - R^2}}, \quad (1)$$

which corresponds to a dipole. Here (R, ϕ) are the polar coordinates on the map, $T_{\text{CMB}} = (2.725 \pm 0.001) \text{ K}$ is the CMB monopole temperature [15], σ_T is Thomson cross section, c is the speed of light, and i is the angle between the line of sight and rotation axis of the ICM. The best observational configuration i.e. the one at which the rotational signal is maximum (corresponding to $i = 90^\circ$), is represented schematically in Fig. 1. It can be seen from Eq. (1) that the two relevant physical quantities in the signal are the radial profiles of the angular velocity, $\omega(r)$, and of the electron number density, $n_e(r)$. To disentangle their contribution to the signal, the electron number density has to be estimated from independent data (e.g. from X-ray photometry). In our case we use the numerical profiles of $n_e(r)$ computed from the simulation data for each cluster, and we fold the corresponding best-fit analytical profiles into Eq. (1). To derive these profiles we fit our data to a simplified six-parameter Vikhlinin model [16]

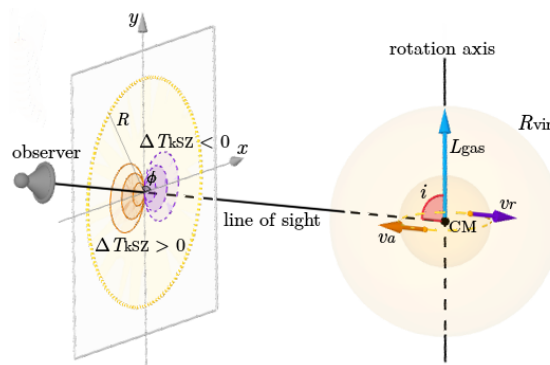


Figure 1. Schematic view illustrating the expected kSZ map from a rotating cluster, assuming the best observational configuration (i.e. with the line of sight orthogonal to the axis of rotation). The gas distribution in the cluster is assumed to be spherically symmetric, with the rotation axis aligned with the angular momentum vector of the gas (L_{gas}). The velocity vectors, v_a and v_r , indicate respectively the approaching and receding velocity components along the line of sight for two generic gas particles, located at the same radial distance from the centre of mass of the cluster.

through a Markov chain Monte Carlo procedure. The angular velocity profile instead, is derived from the so-called vp2b model for the tangential velocity proposed in [13], as follows:

$$\omega(r) = \frac{\text{vp2b}(r)}{r} = \frac{v_{t0}/r_0}{1 + (r/r_0)^2}, \quad (2)$$

therefore $\omega(r)$ depends on the two free parameters, r_0 and v_{t0} , which we want to recover from the fit to the mock kSZ maps.

When the cluster bulk motion is taken into account, and also a rotation is present, the total kSZ signal becomes:

$$\frac{\Delta T_{\text{kSZ}}(R, \phi)}{T_{\text{CMB}}} = \frac{\Delta T_{\text{kSZ,r}}(R, \phi)}{T_{\text{CMB}}} - \frac{\sigma_T}{c} v_{\text{bulk}} \int_R^{R_{\text{vir}}} n_e(r) \frac{2r dr}{\sqrt{r^2 - R^2}}, \quad (3)$$

where $\Delta T_{\text{kSZ,r}}(R, \phi)/T_{\text{CMB}}$ is given in Eq. (1), and v_{bulk} is the projection of the cluster bulk velocity on the line of sight. This additional term produces an asymmetry in the dipole signal given by the rotation, depending on the dominating approaching or receding contribution from v_{bulk} .

3.2. Synthetic maps

We use the `pymSZ`² code to produce the mock maps of our clusters. To compute the maps we simply discretize the signal given by Eq. (3), by summing over the velocity of the gas particles along a given line of sight times the electron density, properly accounting for the projection of the smoothing kernel used in the simulation. To distinguish the rotation-only case, we subtract the average velocity of the gas particles from the single particle velocity. The maps extend over $2.5R_{\text{vir}}$ on each side, with pixel sizes of the order of 10 kpc. The angular size subtended by each pixel is ~ 10 arcsec, which we degrade to a common resolution of 20 arcsec by means of a Gaussian smoothing, in order to emulate observations with a currently operating instrument (e.g. NIKA2 at ~ 200 GHz).

To validate the rotational origin of the dipole signal in our mock kSZ maps, we explore six lines of sight orthogonal to the rotation axis (i.e. fulfilling the condition $i = 0$), at constant steps of 30° ; we label each one of them with the value of the angular separation, θ_{los} , with respect to the reference line of sight (at $\theta_{\text{los}} = 0^\circ$). The dipole produced by rotation is expected to remain unchanged across these different projections, as well as the parameters describing it.

4. Results and discussion

With the aim of recovering the free parameters of the vp2b profile of the tangential velocity introduced in Eq. (2), we calculate a pixel-to-pixel fit to the mock kSZ maps using the two models given by equations (1) (for the rotation-only case) and (3) (for the general case). Fig. 2 illustrates the kSZ maps in the case of cluster 93 (the most massive in the sample), without (Fig. 2a) and with (Fig. 2b) such bulk contribution. Odd columns show the data maps, while even columns show the corresponding best-fit maps. It can be seen that the overall features of the signal are well recovered by our procedure at all the projections. It is also evident how the dipole becomes asymmetric across different lines of sight in the complete case, because of the dominating contribution from the projection of the approaching bulk velocity with respect to the observer. The small-scale outliers in the maps – which are characterized by a signal up to a factor of ~ 3 higher than the best-fit signal – are produced by small high-velocity substructures encountered along the line of sight. Their presence, however, does not affect significantly the

² <https://github.com/weiguangcui/pymSZ>

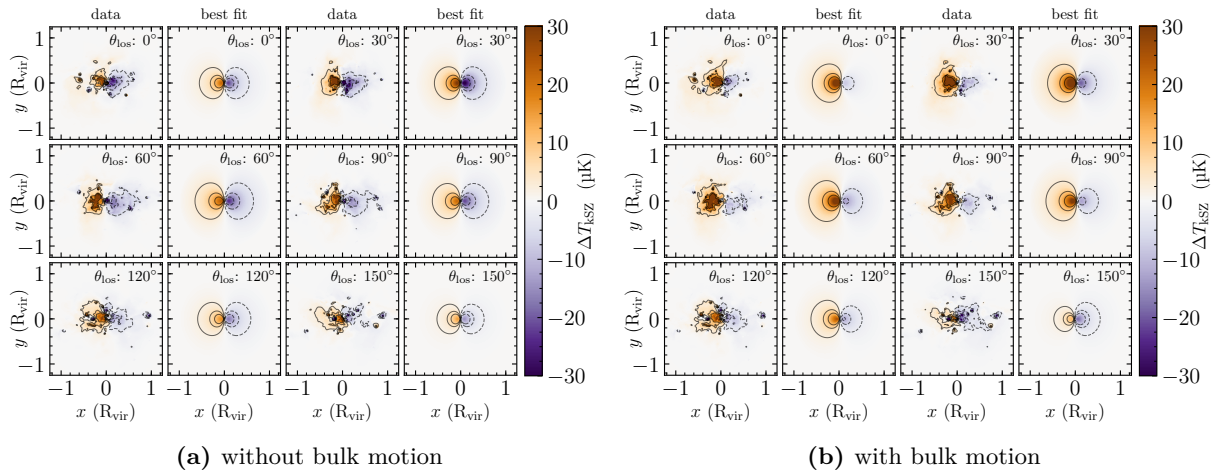


Figure 2. Mock maps of the kSZ temperature distortion for cluster 93, and corresponding best-fit maps, without and with accounting for the cluster bulk velocity (left and right panels, respectively). Contours are plotted from -5σ to 5σ , with dashed (solid) lines for negative (positive) values.

detection of the dipole in terms of amplitude or spatial features. The values of the two free parameters of the rotational model we recover from the fit to the kSZ maps of our cluster sample – r_0 and v_{t0} – are averaged over the explored line of sight. From the comparison of the rotation-only and the rotation+bulk cases, we find agreement within one standard deviation for both parameters. When we compare them to the values from an independent fit to the velocity data from the simulation instead, we get an agreement within at most two-standard deviations for v_{t0} , which is generally overestimated. This could be due to a higher sensitivity of this parameter to the presence of high-velocity outliers located in the outermost regions, or to a non-optimal reconstruction of the signal due to irregularities in the gas density. These results indicate that the vp2b model is, in general, a fairly good description of the tangential velocity profile, and that it is possible to separate the rotational contribution to the signal from the one coming from the bulk motion. This aspect is further confirmed by the lack of significant mutual correlation between the three free parameters, v_{bulk} , r_0 and v_{t0} .

We quantify the rotational signal through the amplitude of the dipole, A_{dip} , measured in the best-fit maps for the rotation-only case. The average values across the different lines of sight are listed in the middle column of Tab. 2: they are of the order of few tens of μK , in agreement with estimates from the literature for relaxed clusters [5]. The right column of Tab. 2 shows the amplitude A_{bulk} of the total kSZ signal given by rotation and bulk, as measured in the

Table 2. Amplitude of the kSZ temperature signal measured from the best-fit maps in the rotation-only case and in the rotation+bulk case (see text).

cluster ID	A_{dip} (μK)	$A_{\text{bulk}}^{\text{max}}$ (μK)
46	10.8 ± 2.5	-57.5
93	21.1 ± 5.2	82.1
98	24.4 ± 9.2	-77.9
103	16.5 ± 2.9	-99.4
205	20.9 ± 5.1	68.8
256	24.4 ± 4.3	-143.1

corresponding best-fit map at the line of sight in which v_{bulk} takes its maximum absolute value. From a comparison between these amplitudes it can be seen that, on average, $A_{\text{dip}}/A_{\text{bulk}}^{\text{max}} \sim 0.23$, therefore a possible measurement of the rotational signal requires high sensitivity, coupled to a sufficiently high angular resolution to detect the dipole at sub-arcminute scales.

To validate our reconstruction of the projected bulk velocity of the clusters, v_{bulk} , we compare the values derived from the fit at different projections with the true values from the simulation data. We find relative differences of the order of few tens per cent between the two at most projections; this indicates that in principle our procedure can be used to constrain the component along the line of sight of the cluster velocity field.

5. Conclusions

We tested the application of the kSZ effect for the detection and the characterization of possible rotational motions in the ICM, using a selected sample of massive and relaxed objects extracted from MUSIC simulations. Assuming the best observational configuration, we computed the synthetic and the theoretical maps of the kSZ temperature distortion assuming only a rotational motion, and also adding the contribution from the cluster bulk motion. In both cases we find a good agreement with the expected model for the rotational velocity, which we also test using the velocity data extracted from the simulations. The rotational signal is found to contribute about 23 per cent of the total maximum kSZ signal, on average, from the study of different lines of sight. Also, the projected cluster bulk velocity and the amplitude of the rotational signal are found to be consistent with the simulation values and with literature expectations, respectively. We are planning to extend this analysis by probing the rotation of ICM in our cluster sample also by means of complementary probes at different wavelengths, and by accounting for instrumental effects by referring to a specific candidate experiment for microwave astronomy.

Acknowledgements

ASB acknowledges funding from Sapienza Università di Roma - Progetti per Avvio alla Ricerca Anno 2017, prot. AR11715C82402BC7.

References

- [1] Biffi V, Dolag K and Böhringer H 2011 *Mon. Not. R. Astron. Soc.* **413** 573–584
- [2] Biffi V *et al.* 2016 *Astrophys. J.* **827** 112
- [3] Bianconi M, Ettori S and Nipoti C 2013 *Mon. Not. R. Astron. Soc.* **434** 1565–1575
- [4] Cooray A and Chen X 2002 *Astrophys. J.* **573** 43–50
- [5] Chluba J and Mannheim K 2002 *Astron. Astrophys.* **396** 419–427
- [6] Sunyaev R A, Norman M L and Bryan G L 2003 *AstL* **29** 783–790
- [7] Hwang H S and Lee M G 2007 *Astrophys. J.* **662** 236–249
- [8] Tovmassian H M 2015 *Astrophysics* **58** 328–337
- [9] Manolopoulou M and Plionis M 2017 *Mon. Not. R. Astron. Soc.* **465** 2616–2633
- [10] Sunyaev R A and Zel’dovich Y B 1970 *Astrophys. Space Sci.* **7** 20–30
- [11] Sunyaev R A and Zel’dovich Y B 1980 *Annu. Rev. Astron. Astrophys.* **18** 537–560
- [12] Sembolini F *et al.* 2013 *Mon. Not. R. Astron. Soc.* **429** 323–345
- [13] Baldi A S *et al.* 2017 *Mon. Not. R. Astron. Soc.* **465** 2584–2594
- [14] Prada F *et al.* 2012 *Mon. Not. R. Astron. Soc.* **423** 3018–3030
- [15] Mather J C *et al.* 1999 *Astrophys. J.* **512** 511–520
- [16] Vikhlinin A *et al.* 2006 *Astrophys. J.* **640** 691–709